Classical and Quantum Gravity

PAPER

Quantum complementarity of clocks in the context of general relativity

To cite this article: Zhifan Zhou *et al* 2018 *Class. Quantum Grav.* **35** 185003

View the article online for updates and enhancements.

You may also like

- How to switch between relational quantum clocks
Philipp A Höhn and Augustin Vanrietvelde
- Probing *f*(*T*) gravity with gravitational time advancement
Xue-Mei Deng
- Atomic clocks for geodesy
Tanja E Mehlstäubler, Gesine Grosche, Christian Lisdat et al.

This content was downloaded from IP address 128.2.149.7 on 04/01/2023 at 19:34

IOP Publishing Classical and Quantum Gravity

Class. Quantum Grav. **35** (2018) 185003 (12pp) https://doi.org/10.1088/1361-6382/aad56b

Quantum complementarity of clocks in the context of general relativity

Zhifan Zhou, Yair Margalit, Daniel Rohrlich[1], Yonathan Japha and Ron Folman

Department of Physics, Ben-Gurion University of the Negev, Be'er Sheva 84105, Israel

E-mail: rohrlich@bgu.ac.il

Received 30 April 2018, revised 5 July 2018
Accepted for publication 24 July 2018
Published 13 August 2018

Abstract

Clocks play a special role at the interface of general relativity and quantum mechanics. We analyze a clock-interferometry thought experiment and go on to theoretically derive and experimentally test a complementarity relation for quantum clocks in the context of the gravitational time lag. The effect of time lag is simulated using a magnetic gradient. We study this relation in detail and discuss its application to various types of quantum clocks.

Keywords: gravitational time dilation, clock interferometry, quantum gravity and proper time, self-interfering quantum clocks, complementarity and gravity, relativistic complementarity

S Supplementary material for this article is available online

(Some figures may appear in colour only in the online journal)

1. Introduction

The interface between quantum mechanics (QM) and general relativity (GR) is an ongoing fundamental challenge. While cosmology and high-energy physics offer tools used for probing this interface and seeking hints for a highly sought-after unification, here our tools are table-top spatial atomic interferometry and atomic clocks. Indeed, progress in matter-wave interferometry [1–3] and atomic clocks [4] has provided a promising platform for new experiments. To unambiguously test the GR notion of proper time in the context of QM, large-scale photon interferometry has been proposed [5, 6], as well as a self-interfering atomic clock [7, 8]. The latter scheme has recently been realized in a proof-of-principle experiment [9]. Quantum complementarity [10] plays a special role at this QM–GR interface, as we show below.

[1] Author to whom any correspondence should be addressed.

 © 2018 IOP Publishing Ltd Printed in the UK

Our present understanding of complementarity [11–15] for a two-path interferometer is summarized by the fundamental inequality $V^2 + D^2 \leqslant 1$, where V is interference pattern visibility and D is distinguishability of the two paths of the interfering particle. This law has been verified in numerous experiments [16–23] and elaborated theoretically [24, 25]. In the framework of GR, there is speculation [7] that the inequality may be broken such that $V^2 + D^2 > 1$. As clock interferometry sensitive to gravitational red shifts may soon be feasible (see [4, 26–30] and table 2 of [7]), formulating an account of clock complementarity is timely. Here we analyze in detail, and test experimentally, a clock complementarity rule for spatial interferometers with internal Hilbert spaces. See also [31] for a closely related analysis. We begin with a clock-interferometry thought experiment, suggesting a clock complementarity rule in the context of proper time. We obtain it theoretically for an atomic clock with two or more internal levels, and verify it empirically in a clock interferometry experiment that includes a simulated gravitational red shift.

2. Theory

In the thought experiment, a clock is prepared in a spatial superposition where one wave packet is closer to a gravitational source and thus suffers from a stronger time lag (or red shift) [7, 9]. We note that it has been theoretically shown that spatial interferometers that are sensitive to a proper time lag between the paths are possible [32]. Now, on the one hand, if the 'ticking' rate of the clock depends on its path, then clock time provides which-path information and the inequality $V^2 + D^2 \leqslant 1$, developed in the framework of non-relativistic QM, must apply. Yet, on the other hand, gravitational time lags do not arise in non-relativistic quantum mechanics, which is not covariant and therefore not consistent with the equivalence principle [33]. Hence our treatment of the clock superposition is a semiclassical extension of quantum mechanics to include gravitational red shifts.

As a historical precedent, we note that at the sixth Solvay conference in 1930, Einstein tried to defeat the uncertainty principle for time and energy by using a clock to measure the precise time a photon is released, and a spring scale to weigh the change in energy E (via $E = mc^2$) of the whole apparatus. Bohr then applied gravitational time dilation to show that Einstein's suggestion could not succeed [34]. Indeed, Bohr's reply to Einstein already contains the idea for our thought experiment, if we transform the uncertain height of the clock in the gravitational potential (during the weighing) into a superposition of the clock at different heights. Yet Bohr's refutation seems, at first sight, mysterious. How could Bohr have applied something outside of quantum mechanics to refute a quantum-mechanical argument? Is not quantum mechanics by itself, without general relativity, a self-consistent theory? The explanation [35] is simple: Einstein suggested measuring the energy of a photon by *weighing* it; he thus equated the *inertial* mass m (in the formula for energy) with the *gravitational* mass (in the weight of the photon). But this equation—the equivalence principle—implies the red shift! In this work we reverse the logical implication: since we impose a red shift, we must also impose the equivalence principle.

According to the equivalence principle, two wave packets traversing an interferometer in a gravitational field can equivalently be described as two wave packets traversing the interferometer and accelerating [36]. That is, we can map the experiment with its gravitational field to an equivalent experiment with no gravitational field, but with acceleration; and relativistic quantum mechanics fully describes the latter experiment. It follows that the two experiments are equivalent; for otherwise, quantum mechanics could distinguish between them, contradicting the equivalence principle. It likewise follows that complementarity, which is expected to hold also for relativistic QM, should also apply to wave packets that acquire different red shifts.

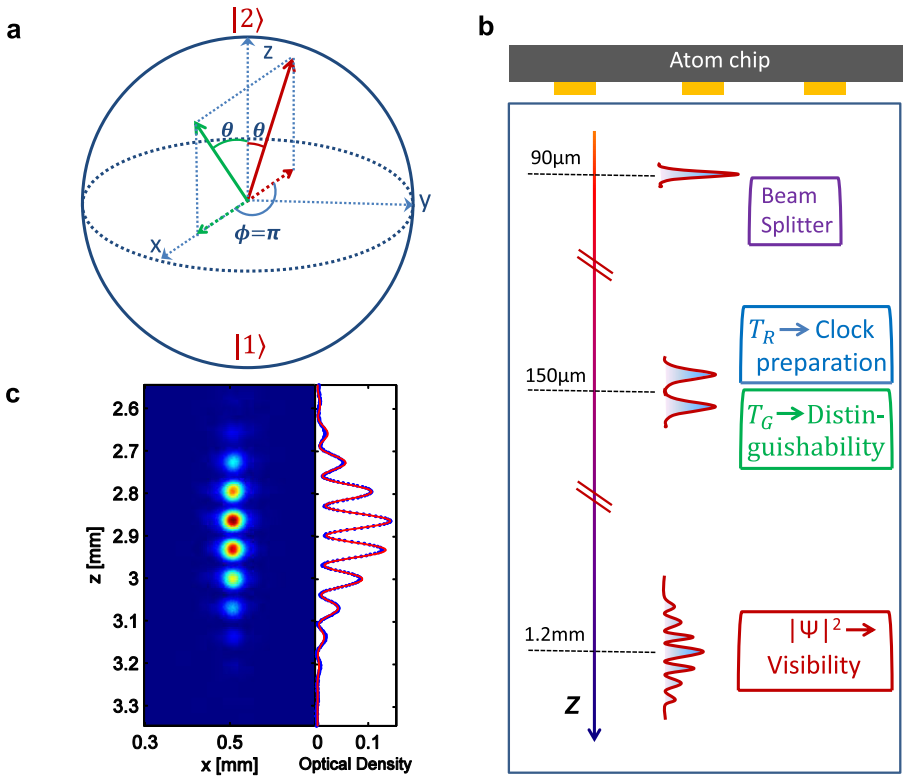

Figure 1. (a) Bloch sphere of the clock interferometer, where the red (green) vector indicates the clock wave packet in the upper (lower) interferometer path. The angle 2θ between the two Bloch vectors (solid lines) is smaller than the angle π between two vectors in a similar interferometer with a perfectly prepared clock (dashed lines). (b) Detailed experimental sequence (not to scale). $C(\theta)$ is controlled by an RF pulse of duration T_{R}. $D_{\mathrm{I}}(\phi)$ is controlled by a magnetic gradient pulse of length T_{G}. (c) 339 experimental shots of the interference pattern in a combined plot (one on top of the other, no alignment or corrections) when $D_{\mathrm{I}}(T_{\mathrm{G}}) = 0$. The visibility is 0.789 ± 0.001. The mean of the single-shot visibility is 0.879 ± 0.002. The errors are standard error of the mean (SEM).

An atomic clock accumulates a quantum phase between two or more internal levels. It is convenient to represent clock states as vectors **s** in the Bloch sphere. In figure 1(a) we show two such vectors corresponding to two interfering clock wave packets. The angle θ corresponds to the clock preparation (and is common to both wave packets) while the angle $\phi = \omega_0 \Delta\tau$ describes the effect of the proper time lapse $\Delta\tau$ between the two clock wave packets, when the clock precesses at rate ω_0 [7, 9]. We consider the case where the distinguishability arises solely from $\Delta\tau$. Because of imperfect clock preparation, $\Delta\tau$ may not increase the distinguishability D to 1 (and correspondingly would not reduce the visibility to zero), and it is useful to characterize the actual distinguishability allowed by the clock by comparing it to the distinguishability D_{I} made possible by a clock with an ideal preparation: full distinguishability $D = 1$ is achieved for $\Delta\phi \equiv \phi_u - \phi_d = \pi$, where u and d denote the upper and lower paths of the interferometer, respectively. We do this by introducing a re-scaling factor C that accounts for such imperfection, taking $D = C \cdot D_{\mathrm{I}}$.

Let us consider a clock that is initially prepared as a superposition $|\theta,\phi\rangle \equiv \cos(\theta/2)|1\rangle + e^{i\phi}\sin(\theta/2)|2\rangle$ of the two clock energy eigenstates $|1\rangle$ and $|2\rangle$. This clock state corresponds to a Bloch vector $\mathbf{s} = (\sin\theta\cos\phi, \sin\theta\sin\phi, \cos\theta)$, which is ideally at $\theta = \pi/2$ on the equator of the Bloch sphere, representing an equal superposition of the two energy eigenstates. After propagation along the two paths, the two clock wave packets acquire an angular difference $\Delta\phi = \omega_0\Delta\tau$ due to the proper time lag. The visibility V of the clock interferometer is equal to the overlap $|\langle u|d\rangle| \equiv |\langle\theta,\phi_u|\theta,\phi_d\rangle|$ between the two states $|u\rangle$ and $|d\rangle$ of the clock wave packets, which have rotated angles ϕ_u and ϕ_d, respectively, during free propagation at different heights in the gravitational field. The angular difference between the two states $|u\rangle$ and $|d\rangle$ makes them distinguishable; the interference visibility is reduced to zero if the overlap between the two states is zero, and the distinguishability $D \equiv \sqrt{1-|\langle u|d\rangle|^2}$ grows to 1, implying full 'which-path' information. In the case of an ideal preparation, where $\cos(\theta/2) = \sin(\theta/2) = 1/\sqrt{2}$, the angular separation between the two Bloch vectors $\mathbf{s}^u$ and $\mathbf{s}^d$ is $\Delta\phi = \phi_u - \phi_d$ and the overlap is $|\langle u|d\rangle| = |\cos(\Delta\phi/2)|$. In general, we can choose two vectors $\mathbf{s}^a$ and $\mathbf{s}^b$ on the Bloch sphere, corresponding to two quantum states $|a\rangle$ and $|b\rangle$, with an angle of separation α_{ab} between them in the plane that they define. Their overlap is likewise $\cos(\alpha_{ab}/2)$. It follows that the distinguishability is

$$D^2 \equiv 1 - |\langle a|b\rangle|^2 = \sin^2(\alpha_{ab}/2) = \frac{1}{2}(1-\cos\alpha_{ab}) = \frac{1}{2}(1-\mathbf{s}^a\cdot\mathbf{s}^b). \tag{1}$$

In our case, where the latitude θ of the clock states does not change over time, the (real) scalar product of the two Bloch vectors $\mathbf{s}^u$ and $\mathbf{s}^d$ is $\mathbf{s}^u\cdot\mathbf{s}^d = \sin^2\theta\cos\Delta\phi + \cos^2\theta$. We use the trigonometric equality $\cos\Delta\phi = 1 - 2\sin^2(\Delta\phi/2)$ and note that $D_\mathrm{I} = |\sin(\Delta\phi/2)|$ is the distinguishability of two states in an ideal clock prepared with the Bloch vector pointing to the equator, namely with equal populations. Upon substituting $\mathbf{s}^u\cdot\mathbf{s}^d$ for $\mathbf{s}^a\cdot\mathbf{s}^b$ in equation (1) we obtain

$$D^2 = \sin^2\theta D_\mathrm{I}^2, \tag{2}$$

namely, the distinguishability of the states of the two clock wave packets is a product of the distinguishability of two states created by perfect preparation of the clock and propagation through the interferometer, scaled by a factor $C = \sin\theta$, which varies from $C = 1$ for an ideal clock to $C = 0$ for a non-clock prepared in a given energy eigenstate (at the north or south pole of the Bloch sphere). While perfect clock preparation ($C = 1$) gives rise to the possibility of perfect distinguishability $D = 1$ (full orthogonality of the clock states) for a given proper time lag $\Delta\tau = \pi/\omega_0$, in the case of imperfect preparation ($C < 1$) the angle between the Bloch vectors of the two wave packets is always smaller than $\alpha_{ud} = \pi$ and the maximum possible distinguishability is $D_\mathrm{max} = C < 1$. (C may be thought of as the clock preparation quality or 'clockness'.) In the context of a clock interferometer [7, 9], where the distinguishability of clock states determines the visibility, the complementarity relation $V^2 + D^2 \leqslant 1$ can now be written as

$$V^2 + (C\cdot D_\mathrm{I})^2 \leqslant 1. \tag{3}$$

This is the clock complementarity relation, where D_I is the ideal clock distinguishability, determined solely by the proper time lag $\Delta\tau$ (in the thought experiment).

The complementarity relation in equation (3) was derived here for a typical atomic clock based on a two-level system. In this case the ideal distinguishability is $D_\mathrm{I}(\Delta\tau) = |\sin(\omega_0\Delta\tau/2)|$ and the clock preparation quality is $C = \sin\theta = 2\sqrt{P(1-P)}$, where P and $1-P$ are the populations (occupation probabilities) of the two energy eigenstates of the clock. In the more

general case—for example, a clock based on an N-level system [spin $S = (N-1)/2$]—we show in section 5 that equation (3) leads to interesting results in which θ and ϕ may not be disentangled when defining C.

In the next section we demonstrate experimentally the complementarity relation of equation (3) with a system of two Zeeman levels of an atom in a magnetic field. A vertical magnetic field gradient $\partial B/\partial z$ takes the place of the gravitational field. The accumulated angular difference between the two clock wave packets centered at heights z_u and z_d is $\phi_u - \phi_d = \Delta\omega_{\text{Zeeman}} T_{\text{G}}$, where T_{G} is the gradient pulse duration and $\Delta\omega_{\text{Zeeman}} = g_F \mu_{\text{B}} (\partial B/\partial z)(z_u - z_d)/\hbar$, μ_{B} is the Bohr magneton and g_F the Landé factor of the hyperfine level F. This clock shift mimics a shift $\omega_0 \Delta\tau$ for a clock in two positions in the gravitational field, where $\Delta\tau \approx g(z_u - z_d)T/c^2$ and T is the time (in the lab frame) during which the two wave packet centers are separated along the axis of gravity.

3. Experimental scheme

We experimentally verify to a high level of likelihood that a two-level clock obeys the generalized clock complementarity rule, with a magnetic gradient simulating a gravitational red shift. The setup used for this study is described in [9], while numerous improvements have resulted in a much higher V in the raw data: figure 1(c) shows very high visibility without any normalization (90% as compared with 60% in [9]). The experimental scheme is depicted in figure 1(b); it applies the previously demonstrated Stern–Gerlach (SG) matter-wave interferometer on an atom chip [41] in the following experimental sequence. (For more details, see the supplementary material (stacks.iop.org/CQG/35/185003/mmedia).) A BEC of about 10^4 ^{87}Rb atoms in the state $|F, m_F\rangle = |2, 2\rangle$ is released from a magnetic trap located 90 ± 2 μm below the chip surface; next, after 0.9 ms, the SG beam splitter acts on it. It creates a coherent spatial superposition of two wave packets in the same spin state ($|2, 2\rangle$). A stopping pulse then adjusts the relative velocity of the two wave packets so that they have the same momentum. With zero relative velocity, the two clock wave packets overlap during time-of-flight (TOF) free expansion and create spatial interference fringes. Clocks are prepared by an RF pulse of duration T_{R}, which creates a superposition of $|2, 2\rangle \equiv |2\rangle$ and $|2, 1\rangle \equiv |1\rangle$ states. The pulses are applied under a strong homogeneous magnetic field (36.7 G) in order to push the transition to $|2, 0\rangle$ out of resonance via the nonlinear Zeeman effect, thus forming a pure two-level system. As the Rabi frequency Ω_{R} is constant, varying T_{R} will effectively change the Bloch vector's polar angle θ in the Bloch sphere (figure 1(a)), e.g. when $T_{\text{R}} = 0$ μs, there is no rotation and the Bloch vector stays at the north pole, and when $T_{\text{R}} = 10$ μs, the Bloch vector is rotated onto the equator and a proper clock is prepared in the state $(|2\rangle + |1\rangle)/\sqrt{2}$. Then an additional magnetic gradient pulse of duration T_{G} is applied in order to change the relative 'tick' rate of the superposed clock wave packets, thus determining a relative rotation ϕ on the equator of Bloch sphere (figure 1(a)). This synthetic red shift introduces *a posteriori* which-path information (WPI) by creating entanglement between the path and a WPI marker, in contrast to the *a priori* WPI, which involves the preparation of an unbalanced interferometer such that the particle flux along the two paths differs. An image is taken (in the xz plane) after the wave packets expand and overlap. (The absorption imaging is insensitive to the Zeeman states, i.e. $|1\rangle$ and $|2\rangle$ count equally.) Because two BEC wave packets are always expected to yield fringes when they overlap, many experimental cycles are required in order to prove phase stability or, in other words, coherent splitting of the clock.

Let us note that it is not enough to experimentally simulate the thought experiment by placing a clock in a spatial superposition, and creating a synthetic red shift with some force field.

To faithfully simulate the thought experiment one must make sure that there is no breakup of the clock due to the applied force field. This may be viewed as a mere technical condition for the operation of a clock, but in fact the 'no clock breakup' is a fundamental feature of the thought experiment that must be imitated by any experimental simulation. Specifically, there is no breakup of a clock wave packet in the gravitational field. Consider a *single* wave packet centered at a point z_0 and let $\tau(z_0)$ be a proper time lapse there. While two clock levels are indeed accelerated in the gravitational field to different momenta $p_j = m_j g\tau(z_0)$ (where the mass difference $m_2 - m_1 = \hbar\omega_0/c^2$ is due to the difference $\hbar\omega_0$ in their energies), the corresponding velocities $v_j = p_j/m_j = g\tau(z_0)$ do not depend on the specific clock level. The Galilean law of falling masses, stating that gravitational acceleration is independent of mass, holds in general relativity and insures that clock breakup will not occur in a gravitational field. Similarly, the clock breakup effect in our experiment is negligible relative to the difference of the clock angle between the two clock wave packets. A clock wave packet $\psi_0(z)(|1\rangle + |2\rangle)$ in a magnetic field gradient undergoes not only a rotation of the clock $|1\rangle + |2\rangle \to |1\rangle e^{-i\omega_1 T_G} + |2\rangle e^{-i\omega_2 T_G}$, where ω_1 and ω_2 are the magnetic potentials for the two levels at z_0, but also a differential momentum. While the differential clock rotation is shown to span a large range of clock angles allowing the two clock states to be fully distinguishable ($D_I = 1$), the momentum separation between the two states of the same clock, which is given by $\Delta p = \hbar(\partial\omega_1/\partial z - \partial\omega_2/\partial z)T_G$, is much smaller than the momentum distribution of each wave packet (allowing the observation of many spatial fringes [9]). These conditions are automatically fulfilled in our experiment when the separation between the two wave packets is larger than the wave packet width. It follows that our demonstration of the effect of gravitational red shift on clock distinguishability is valid.

4. Verifying clock complementarity

Each clock is a superposition of two Zeeman sublevels $|1\rangle \equiv |2,1\rangle$ and $|2\rangle \equiv |2,2\rangle$, with coefficients that depend on θ and ϕ. The RF pulse (duration T_R) controls the value of $C = \sin\theta$, while the magnetic gradient pulse (duration T_G) controls the value of $D_I = \sin(\phi/2)$. The latter creates an effective red shift, namely a differential clock 'tick' rate, by inducing a differential Zeeman splitting $\Delta\omega$ such that $\phi = \Delta\omega \cdot T_G$. Finally V is measured from the spatial interference pattern (figure 1(c)). We measure $C^2 = 4P(1-P)$ independently in a separate experiment by measuring P after the clock is initialized, and we evaluate D_I independently by measuring the relative phases in two single-state interferometers, one for each of the two clock states.

The independent measurements of V, C and D_I are presented in figure 2. As noted, $C = \sin\theta = 2\sqrt{P(1-P)}$, and in order to establish the value of C we need to measure the population transfer from the $m_F = 2$ state to the $m_F = 1$ state. In figure 2(a) we show the population transfer measured by Stern–Gerlach splitting of the different spin states and atom counting, and figure 2(b) shows the resulting value of C^2. As expected, C^2 oscillates between 0 and 1, corresponding to the population transfer. In figure 2(c), we scan T_G and measure the optimal clock ($C = 1$) interference visibility. The result is fitted with $|\cos(\phi/2)|$, where ϕ represents the clock relative rotation. In figures 2((d)–(f)) D_I is measured by two single-state interferometers ($m_F = 2$ and $m_F = 1$). The difference in phase between these two interferometric fringe patterns is equivalent to the relative rotation ϕ between the upper and lower clock wave packets, from which D_I is directly calculated as $|\sin(\phi/2)|$. The measured relations among the population transfer P, the parameter C^2 and the visibility V appear in greater detail in figure 3, for the case of D_I equal to 1.

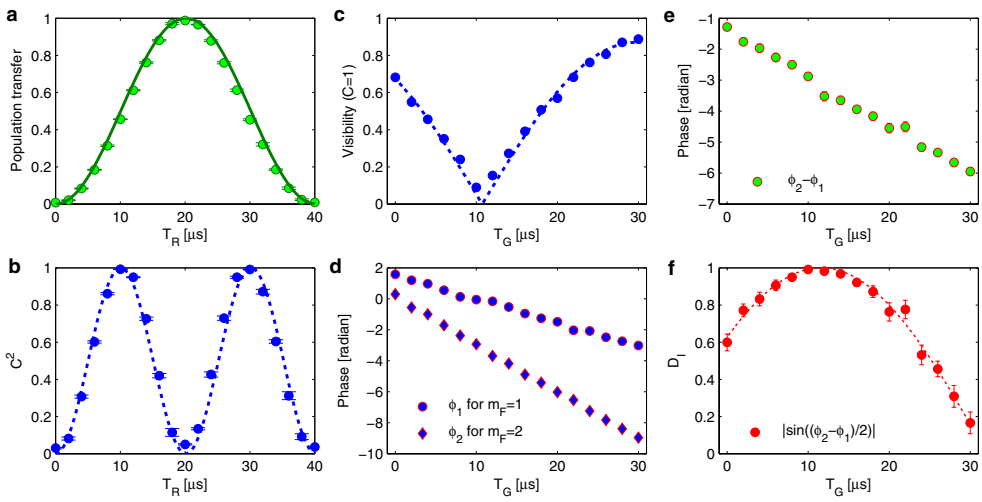

Figure 2. The independent measurement of V, C and D_{I}: ((a) and (b)) $C^2 = 4P(1-P)$ is measured independently in a separate experiment by measuring the population transfer P after the clock is prepared by an RF pulse of duration T_{R}; (c) the visibility of an ideal clock ($C = 1$) interference pattern versus T_{G}, which induces distinguishability; the result is fitted to $|\cos(\phi/2)|$. ((d)–(f)) D_{I} is evaluated independently by measuring the relative angle in two single-state interferometers each containing one of the two clock states, ϕ_1 for $m_F = 1$ and ϕ_2 for $m_F = 2$, and then by calculating $D_{\mathrm{I}} = |\sin(\phi_2 - \phi_1)/2|$. The errors are standard error of the mean (SEM) and are at times not visible because of their small magnitude.

In figure 4(a) we present the clock complementarity relation $V^2 + (C \cdot D_{\mathrm{I}})^2$ for four values of C when D_{I} is scanned. Figure 4(b) presents the clock complementarity for four values of D_{I} when C is scanned. With V, C and D_{I} measured independently, figure 4 demonstrates that the clock complementarity rule is sound.

5. Multilevel clocks

To achieve an atomic clock with a better time precision it is possible to choose a pair of energy eigenstates with a larger energy spacing $\hbar\omega_0$. In the context of our Zeeman level clock it is possible, for example, to prepare the system as a superposition of the two extreme Zeeman levels $m_F = \pm 2$ of the $F = 2$ manifold and use this system as a two-level clock with rotation frequency $2F\omega_0$. (See [42] for a possible realization.) The discussion in section 2 is valid for this system exactly in the same way.

An example of a multilevel clock where a few or many levels are occupied simultaneously during the clock evolution provides a model for examining the transition to the classical clock limit where the clock hand moves over a continuum of distinguishable times. So far, a two-level clock was prepared by using a Rabi rotation that places the $S = 1/2$ Bloch vector at an angle θ from the z axis of the Bloch sphere. Let us consider an $S > 1/2$ system prepared in a similar way. (For an example of such a preparation see [43]; for a possible realization of a very large S see [44].) Figures 5((a) and (b)) show an $S = 8$ clock interferometer on the Bloch sphere. In a spin-S system (with $N = 2S + 1$ levels and equal energy spacing), one may rotate the state along the θ direction while free evolution rotates the state along the ϕ direction. As in the spin-1/2 system, the overlap between two states $|\theta_a, \phi_a\rangle$ and $|\theta_b, \phi_b\rangle$, representing two

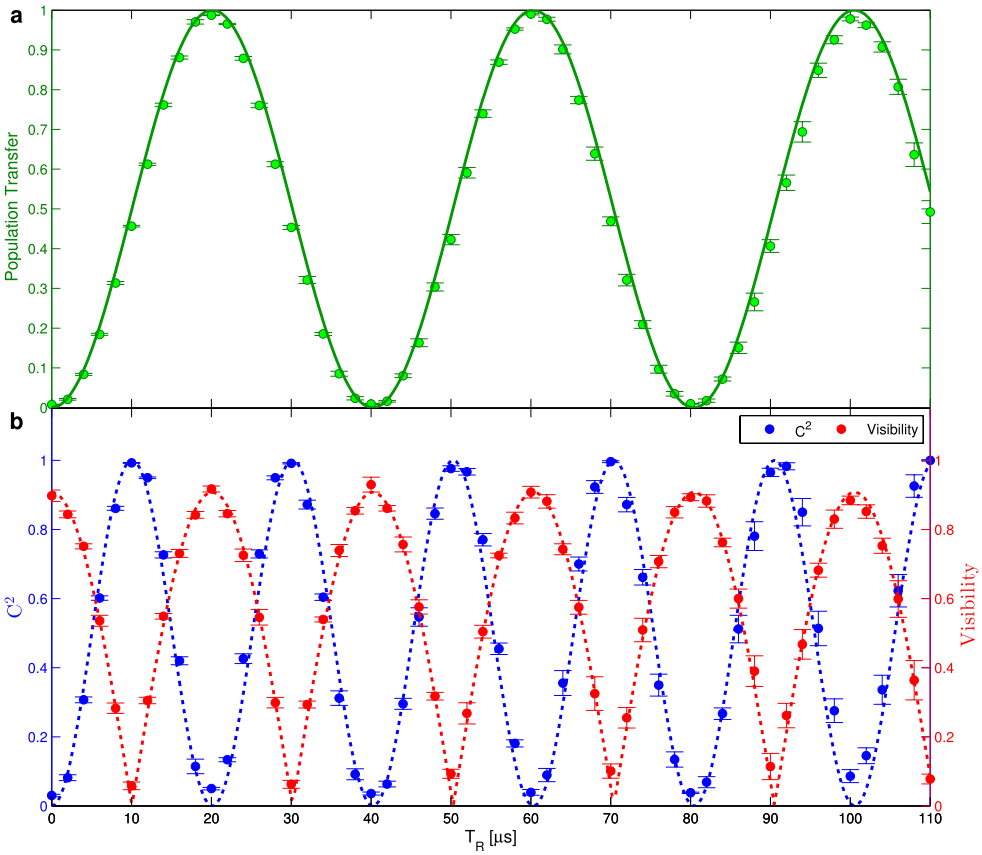

Figure 3. (a) Clock preparation, showing the population transfer P versus T_{R}. (b) In blue, the measured C^2 versus T_{R}, when $\Delta\phi = \pi$ (and $D_{\mathrm{I}} = 1$ with an uncertainty of 1%), as well as (dashed line) the calculated $C^2 = 4P(1-P)$, taking P from (a). For reference, we also show (in red) the measured V versus T_{R}, as well as (dashed line), the calculated visibility $V = |\cos\theta| V_{\max} = |1-2P| V_{\max}$ (again, taking P from (a)), where $V_{\max} = 0.9$ is our maximal visibility limited by optical resolution, etc. The figure shows the complementary between C^2 and V when D_{I} equals 1.

coherent states obtained by such rotations starting from the extreme energy eigenstate $m_S = S$, is determined by the angle α_{ab} between the two Bloch vectors $\mathbf{s}^a$ and $\mathbf{s}^b$ corresponding to the two quantum states. For example, consider the overlap between the two states $|\theta_a, \phi_a\rangle = |0,0\rangle$ (the extreme energy eigenstate on the north pole) and $|\theta,\phi\rangle$ obtained by a Rabi rotation of the state $|0,0\rangle$ with an angle θ. This state has the form

$$|\theta,\phi\rangle = \sum_{m=-S}^{S} \cos^{S+m}(\theta/2)\sin^{S-m}(\theta/2)\sqrt{\binom{2S}{S+m}}\,\mathrm{e}^{-\mathrm{i}m\phi}|S,m\rangle, \tag{4}$$

where $|S,m\rangle$ are the spin eigenstates and $\binom{2S}{S+m}$ are binomial coefficients for choosing $S+m$ out of $2S+1$. It follows that the overlap integral is given by $|\langle 0,0|\theta,\phi\rangle| = \cos^{2S}(\theta/2)$. As rotations around the Bloch sphere are unitary operations and do not change the overlap between two states transformed under the same operation, and as can be verified directly

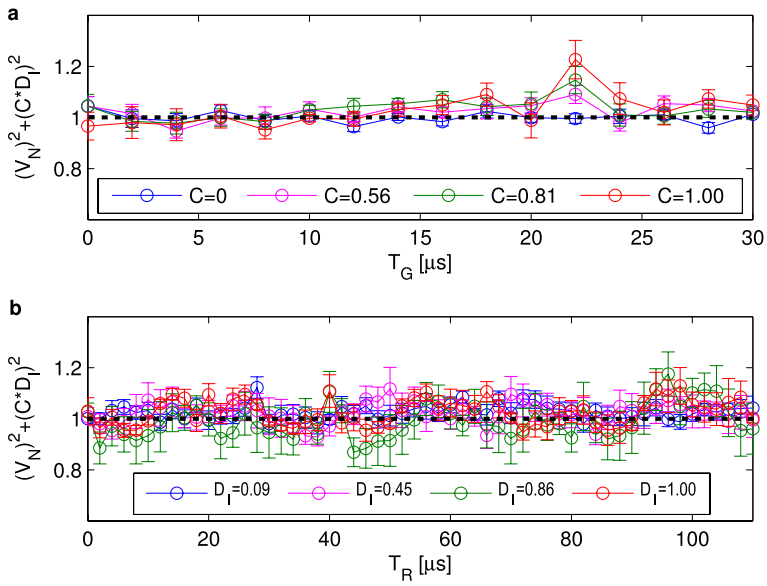

Figure 4. The value of $V_N^2 + (C \cdot D_I)^2$, where all three parameters are measured independently: (a) for four values of C when D_I is scanned, and (b) for four values of D_I when C is scanned. V_N is the normalized visibility: each value of the visibility is an average of the single-shot visibility from several experimental cycles, and the error bars represent the standard error of the mean (SEM) in this sub-sample. For error bars corresponding to standard deviation (SD) we multiply by $\sqrt{n}$, where $n = 6$ is the number of data points. This average is normalized to the visibility of the single-state interferometer (i.e. without an initialization of a clock) to account for experimental imperfections. In figure 4(a), the value at T_G near 22 μs originates from a relatively large experimental error in measuring the interferometric phase, as can be seen in figures 2((d)–(f)). However, these values are still within one standard deviation of the value 1.

from the above equation, we can generalize this result to any two coherent states on the Bloch sphere, such that

$$|\langle \theta_a, \phi_a | \theta_b, \phi_b \rangle| = \cos^{2S}(\alpha_{ab}/2), \tag{5}$$

where α_{ab} is the angle between the two Bloch vectors such that $\cos \alpha_{ab} = \mathbf{s}^a \cdot \mathbf{s}^b$. By using some trigonometric equations we conclude that for two Bloch vectors prepared at the same latitude θ the distinguishability is

$$D^2 = 1 - \left[\frac{1}{2}(1 + \mathbf{s}^u \cdot \mathbf{s}^d)\right]^{2S} = 1 - [1 - \sin^2\theta \sin^2(\Delta\phi/2)]^{2S}. \tag{6}$$

For $S = 1/2$ this leads to the same expression as in equations (1) and (2). The ideal distinguishability is $D_I^2 = 1 - \cos^{4S}(\Delta\phi/2)$ (conforming to the two-level system result for $S = 1/2$). This implies that the 'clockness' C should be

$$C^2 \equiv \frac{D^2}{D_I^2} = \frac{1 - [1 - \sin^2\theta \sin^2(\Delta\phi/2)]^{2S}}{1 - \cos^{4S}(\Delta\phi/2)}. \tag{7}$$

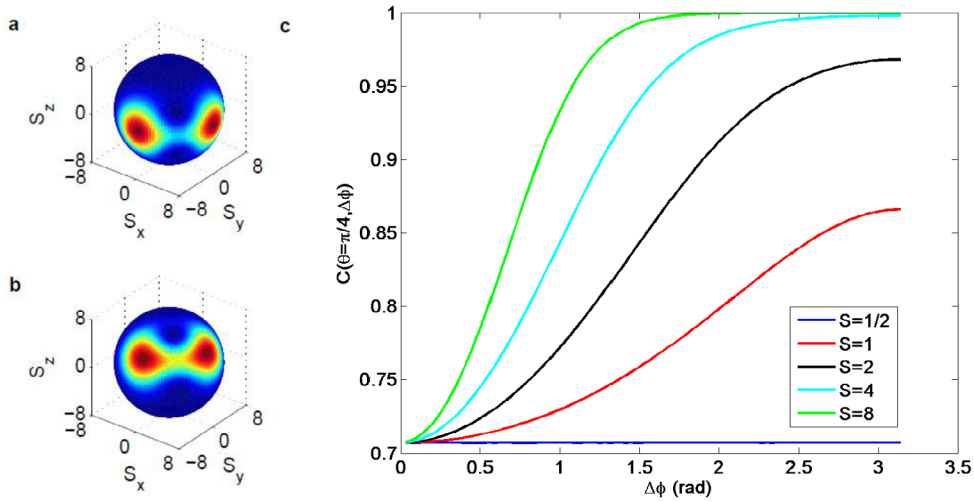

Figure 5. Distinguishability for coherent states of spin $S \geqslant 1/2$. (a) The Bloch sphere of $S = 8$ showing the angular distribution of a superposition of states $|\theta, \phi\rangle = |\pi/2, 0\rangle$ and $|\pi/2, -\pi/2\rangle$ with almost full distinguishability. (b) A similar superposition for a non-ideal clock prepared at $\theta = \pi/3$; the two states show a considerable overlap. (c) 'Clockness' C for a preparation angle $\theta = \pi/4$ as a function of the phase difference $\Delta\phi$ and different spin values S. For $\Delta\phi \to 0$ $C \to \sin\theta$ is independent of spin, but for large $\Delta\phi$ the 'clockness' is large for large spins as the angular distribution on the Bloch sphere is narrow, implying high distinguishability regardless of the preparation angle.

In the limit of a very short time lag $\Delta\phi \to 0$, the 'clockness' becomes $C \to \sin\theta$, the same as for spin-1/2 and independent of the spin. However, for general proper time lags of the two clocks, C becomes dependent both on the spin S and the angle difference $\Delta\phi$. The value of C as a function of $\Delta\phi$ is shown in figure 5(c). For large values of the spin S and large proper time differences, the distinguishability is no longer sensitive to the clock preparation angle, as the clock states are represented by a narrow distribution of angles on the Bloch sphere and therefore two states with large $\Delta\phi$ are well separated even if the preparation angle is not ideal.

Finally, we can apply the clock complementarity relation in equation (3) to a single-state spatial interferometer, e.g. the Compton clock for which $C = 0$; [37–40]; but $C = 0$ does not correspond to a clock in the usual sense of an internal state space. What is unique to $C > 0$ clock interferometry is the reduced V due to different clock readings along the paths, rendering the paths distinguishable [7, 9]. An additional implication of equations (1) and (2) is that $V^2 + D^2 > 1$ [7] requires either $V \neq |\langle \mathbf{s}^u | \mathbf{s}^d \rangle|$ or new rules for scalar products in quantum mechanics.

6. Conclusion

In summary, we have theoretically obtained and experimentally confirmed a clock complementarity relation, $V^2 + (C \cdot D_\mathrm{I})^2 = 1$, for clock wave packets superposed on two paths through an interferometer. Here V is the visibility of their interference pattern, C is a measure of the 'preparation quality' of the clock, and D_I is the distinguishability of an ideally prepared clock. We emphasize that our experiment measures V, C, D_I independently. While this relation is specific to clock complementarity, it is unusual in linking non-relativistic quantum

mechanics with general relativity. A direct test of this complementarity relation will come when D_{I} reflects the gravitational red shift between two paths which traverse different heights.

Acknowledgments

We gratefully acknowledge discussions with Wolfgang Schleich and Albert Roura. We thank Zina Binstock for the electronics and the BGU nano-fabrication facility for providing the high-quality chip. This work is funded in part by the Israel Science Foundation (grant no. 1381/13), the EC Matter-Wave consortium (FP7-ICT-601180), and the German-Israeli DIP project (Hybrid devices: FO 703/2-1) supported by the DFG. We also acknowledge support from the Israeli Council for Higher Education and from the Ministry of Immigrant Absorption (Israel). DR thanks the John Templeton Foundation (Project ID 43297) and the Israel Science Foundation (grant no. 1190/13) for support. The opinions expressed in this publication do not necessarily reflect the views of the John Templeton Foundation.

ORCID iDs

Daniel Rohrlich https://orcid.org/0000-0002-6252-3048

References

[1] Kovachy T *et al* 2015 Quantum superposition at the half-metre scale *Nature* **528** 530–3
[2] Muntinga H *et al* 2013 Interferometry with Bose–Einstein condensates in microgravity *Phys. Rev. Lett.* **110** 093602
[3] Yu C, Estey B, Zhong W, Parker R H and Müller H 2016 Improved accuracy of atom interferometry using Bragg diffraction *Proc. of the 7th Meeting on CPT and Lorentz Symmetry* (Bloomington, IN: Indiana University) (https://doi.org/10.1142/9789813148505_0001)
[4] Nicholson T L *et al* 2015 Systematic evaluation of an atomic clock at 2×10^{-18} total uncertainty *Nat. Commun.* **6** 6896
[5] Zych M *et al* 2012 General relativistic effects in quantum interference of photons *Class. Quantum Grav.* **29** 224010
[6] Pallister S *et al* 2017 A blueprint for a simultaneous test of quantum mechanics and general relativity in a space-based quantum optics experiment *EPJ Quantum Technol.* **4** 2
[7] Zych M, Costa F, Pikovski I and Brukner Č 2011 Quantum interferometric visibility as a witness of general relativistic proper time *Nat. Commun.* **2** 505
[8] Bushev P A, Cole J H, Sholokhov D, Kukharchyk N and Zych M 2016 Single electron relativistic clock interferometer *New J. Phys.* **18** 093050
[9] Margalit Y *et al* 2015 A self-interfering clock as a 'which path' witness *Science* **349** 1205
[10] Bohr N 1928 Das quantenpostulat und die neuere entwicklung der atomistik *Naturwissenschaften* **16** 245
[11] Englert B-G 1996 Fringe visibility and which-way information: an inequality *Phys. Rev. Lett.* **77** 2154
[12] Greenberger M D and Yasin A 1988 Simulteneous wave and particle knowledge in a neutron interferometer *Phys. Lett.* A **128** 391
[13] Jaeger G, Shimony A and Vaidman L 1995 Two interferometric complementarities *Phys. Rev.* A **51** 54
[14] Mandel L 1991 Coherence and indistinguishability *Opt. Lett.* **16** 1882
[15] Wootters W K and Zurek W H 1979 Complementarity in the double-slit experiment: quantum nonseparability and a quantitative statement of Bohr's principle *Phys. Rev.* D **19** 473
[16] Jacques V *et al* 2008 Delayed-choice test of quantum complementarity with interfering single photons *Phys. Rev. Lett.* **100** 220402

[17] Durr S, Nonn T and Rempe G 1998 Fringe visibility and which-way information in an atom interferometer *Phys. Rev. Lett.* **81** 5705
[18] Summhammer J, Badurek G, Rauch H, Kischko U and Zeilinger A 1983 Direct observation of fermion spin superposition by neutron interferometry *Phys. Rev.* A **27** 2523
[19] Zou X Y, Wang L J and Mandel L 1991 Induced coherence and indistinguishability in optical interference *Phys. Rev. Lett.* **67** 318
[20] Bertet P *et al* 2001 A complementarity experiment with an interferometer at the quantum-classical boundary *Nature* **411** 166
[21] Buks E, Schuster R, Heiblum M, Mahalu D and Umansky V 1998 Dephasing in electron interference by a 'which-path' detector *Nature* **391** 871
[22] Pfau T, Spalter S, Kurtsiefer C, Ekstrom C R and Mlynek J 1994 Loss of spatial coherence by a single spontaneous emission *Phys. Rev. Lett.* **73** 1223
[23] Chapman M S *et al* 1995 Photon scattering from atoms in an atom interferometer: coherence lost and regained *Phys. Rev. Lett.* **75** 3783
[24] Englert B-G and Bergou J 2000 Quantitative quantum erasure *Opt. Commun.* **179** 337
[25] Banaszek K, Horodechi P, Karpinski M and Radzewicz C 2013 Quantum mechanical which-way experiment with an internal degree of freedom *Nat. Commun.* **4** 2594
[26] Chou C W, Hume D B, Rosenband T and Wineland D J 2010 Optical clocks and relativity *Science* **329** 1630
[27] Campbell S L *et al* 2017 A Fermi-degenerate three-dimensional optical lattice clock *Science* **358** 90
[28] Huntemann N, Sanner C, Lipphardt B, Tamm C and Peik E 2016 Single-ion atomic clock with 3×10^{-18} systematic uncertainty *Phys. Rev. Lett.* **116** 063001
[29] Chen J-S, Brewer S M, Chou C W, Wineland D J, Leibrandt D R and Hume D B 2017 Sympathetic ground-state cooling and time-dilation shifts in an $^{27}Al^{+}$ optical clock *Phys. Rev. Lett.* **118** 053002
[30] Ludlow A D, Boyd M M, Ye J, Peik E and Schmidt P O 2015 Optical atomic clocks *Rev. Mod. Phys.* **87** 637
[31] Pikovski I, Zych M, Costa F and Brukner Č 2017 Time dilation in quantum systems and decoherence *New J. Phys.* **19** 025011
[32] Greenberger D M, Schleich W P and Rasel E M 2012 Relativistic effects in atom and neutron interferometry and the differences between them *Phys. Rev.* A **86** 063622
[33] Lugli M 2017 Mass and proper time as conjugated observables *Graduate Thesis* University of Pavia, Pavia (arXiv: 1710.06504 [quant-ph])
[34] Bohr N 1951 Discussions with Einstein on epistemological problems in atomic physics *Albert Einstein: Philosopher–Scientist*, ed P A Schilpp (New York: Tudor Pub. Co.) pp 201–41
[35] Aharonov Y and Rohrlich D 2005 *Quantum Paradoxes: Quantum Theory for the Perplexed* (Weinheim: Wiley-VCH) section 2.4
[36] Feynman R, Leighton R and Sands M 1963 *The Feynman Lectures on Physics* vol I (Reading, MA: Addison-Wesley) section 42–6
[37] Lan S-Y *et al* 2013 A clock directly linking time to a particle's mass *Science* **339** 554
[38] Wolf P *et al* 2011 Does an atom interferometer test the gravitational redshift at the Compton frequency? *Class. Quantum Grav.* **28** 145017
[39] Schleich W P, Greenberger D M and Rasel E M 2013 Redshift controversy in atom interferometry: representation dependence of the origin of phase shift *Phys. Rev. Lett.* **110** 010401
[40] Peil S and Ekstrom C R 2014 Analysis of atom-interferometer clocks *Phys. Rev.* A **89** 014101
[41] Machluf S, Japha Y and Folman R 2013 Coherent Stern–Gerlach momentum splitting on an atom chip *Nat. Commun.* **4** 2424
[42] Lovecchio C *et al* 2016 Optimal preparation of quantum states on an atom-chip device *Phys. Rev.* A **93** 010304
[43] Petrovic J, Herrera I, Lombardi P, Schaefer F and Cataliotti F S 2013 A multi-state interferometer on an atom chip *New J. Phys.* **15** 043002
[44] Derek F, Kimball J, Sushkov A O and Budker D 2016 Precessing ferromagnetic needle magnetometer *Phys. Rev. Lett.* **116** 190801